

See discussions, stats, and author profiles for this publication at: <https://www.researchgate.net/publication/45826360>

Proliferation Inhibition, DNA Damage, and Cell-Cycle Arrest of Human Astrocytoma Cells after Acrylamide Exposure

ARTICLE *in* CHEMICAL RESEARCH IN TOXICOLOGY · SEPTEMBER 2010

Impact Factor: 3.53 · DOI: 10.1021/tx1000893 · Source: PubMed

CITATIONS

10

READS

28

4 AUTHORS, INCLUDING:



Tsui-Chun Tsou

National Health Research Institutes

65 PUBLICATIONS 1,206 CITATIONS

SEE PROFILE



Ing-Ming Chiu

National Health Research Institutes

136 PUBLICATIONS 3,785 CITATIONS

SEE PROFILE



Chin-Cheng Chou

National Taiwan University

32 PUBLICATIONS 294 CITATIONS

SEE PROFILE

Proliferation Inhibition, DNA Damage, and Cell-Cycle Arrest of Human Astrocytoma Cells after Acrylamide Exposure

Jong-Hang Chen,[†] Tsui-Chun Tsou,[‡] Ing-Ming Chiu,^{§,||} and Chin-Cheng Chou^{*,†,⊥}

Department of Veterinary Medicine, National Taiwan University, No. 1, Sec. 4, Roosevelt Road, Taipei 106, Taiwan, Division of Environmental Health and Occupational Medicine, National Health Research Institutes, 35 Keyan Road, Zhunan, Miaoli County 350, Taiwan, Institute of Cellular and System Medicine, National Health Research Institutes, 35 Keyan Road, Zhunan, Miaoli County 350, Taiwan, Department of Internal Medicine, The Ohio State University, 480 West Ninth Avenue, Columbus, Ohio 43210, and Center for Zoonoses Research, College of Bio-Resources and Agriculture, National Taiwan University, No. 1, Sec. 4, Roosevelt Road, Taipei 106, Taiwan

Received March 9, 2010

Acrylamide (ACR) has been recognized as a neurological and reproductive toxin in humans and laboratory animals. This study aimed to determine the effects of ACR-induced DNA damage on cell cycle regulation in human astrocytoma cell lines. Treatment of U-1240 MG cells with 2 mM ACR for 48 h resulted in a significant inhibition of cell proliferation as evaluated by Ki-67 protein expression and MTT assay. The analysis of DNA damage with the comet assay showed that treatment of the cells with 0.5, 1, and 2 mM ACR for 48 h caused significant increases in DNA damage by 3.5-, 4-, and 14-fold, respectively. Meanwhile, analysis of cell-cycle arrest with flow cytometry revealed that the ACR treatments resulted in significant increases in the G₀/G₁-arrested cells in a time- and dose-dependent manner. Expression of DNA damage-associated/checkpoint-related signaling molecules, including phosphorylated-p53 (pp53), p53, p21, p27, Cdk2, and cyclin D₁, in three human astrocytoma cell lines (U-1240 MG, U-251 MG, and U-87 MG) was also analyzed by immunoblotting. Treatment of the three cell lines with 2 mM ACR for 48 h caused marked increases in pp53 and Cdk2, as well as decreases in cyclin D₁ and p27. Moreover, increases in p53 and p21 were detected in both U-1240 and U-87 MG cells, whereas no marked change in p53 and a decrease in p21 were observed in U-251 MG cells. To address the involvement of ataxia telangiectasia mutated/ATM-Rad3-related (ATM/ATR) kinase in the signaling of ACR-induced G₀/G₁ arrest, caffeine was used to block the ATM/ATR pathway in U-1240 MG cells. Caffeine significantly attenuated the ACR-induced G₀/G₁ arrest as well as the expression of DNA damage-associated/checkpoint-related signaling molecules in a dose-dependent manner. This in vitro study clearly demonstrates the critical role of ATM/ATR in the signaling of ACR-induced cell-cycle arrest in astrocytoma cells.

Introduction

Acrylamide (ACR) is a water-soluble vinyl monomer and has many applications in industries and protein analysis (1). ACR can be found in food processed at high temperatures (2) and has neurological and reproductive toxicities to humans and laboratory animals (3, 4). The International Agency for Cancer Research suggests that ACR is a “probable human carcinogen” (5). ACR increases tumor incidence at multiple sites upon exposure in animals (6, 7). In humans, dietary ACR intake has positive associations with the risk of endometrial, ovarian, and renal cancer but not with brain cancer (8).

The toxic effects of ACR on neurons have been investigated intensively, including the reduction of cell viability, the induction of apoptosis and p53 phosphorylation (9, 10), the formation of perikaryal inclusion bodies (11), and the transduction of neurodegeneration-related signals (12). Few studies related to

glial cells have been reported. No significant effects of ACR on cytotoxicity and cell proliferation have been found for primary culture of rat or human astrocytoma cell lines (U-251 MG, U-373 MG, and CCF-STTG1) after exposure to ACR up to 24 h (13–16). However, our previous study indicated that ACR treatments not only caused cytotoxicity but also induced astrogliotic and apoptotic responses in the human astrocytoma U-1240 MG cells (17). Because astrocytes play an important role in maintaining the normal functions of CNS (18, 19), it is critical to further determine the molecular mechanisms of ACR's effects on astrocytes.

ACR has been reported to induce DNA damage in various cells by the comet assay and the micronucleus test (20–24). Upon DNA damage, ataxia telangiectasia mutated (ATM) and ATM-Rad3-related (ATR) kinases participate in the activation of cell-cycle checkpoints (25). In response to DNA damage, ATM and ATR induce the phosphorylation of p53 at Ser-15, which promotes the accumulation and functional activation of p53 (26) and thus leads to cell-cycle arrest and apoptosis (27).

To the best of our knowledge, studies in ACR exposure on DNA damage and its resulting cell-cycle arrest of astrocytic cells remain lacking. Human astrocytoma U-1240 MG cells exhibit toxic responses to ACR exposure (17). Thus, this study chose U-1240 MG cells to investigate the effects of ACR on cell proliferation and DNA damage, as well as to determine

* Corresponding author. Tel: +886-2-3366-1292. Fax: +886-2-2363-0495. E-mail: chouchin@ntu.edu.tw.

[†] Department of Veterinary Medicine, National Taiwan University.

[‡] Division of Environmental Health and Occupational Medicine, National Health Research Institutes.

[§] Institute of Cellular and System Medicine, National Health Research Institutes.

^{||} The Ohio State University.

[⊥] Center for Zoonoses Research, National Taiwan University.

the regulatory mechanism of cell-cycle arrest via the ATM/ATR-mediated activations of checkpoint-related signals. In this study, the MTT assay and immunofluorescence staining of Ki-67 protein were used to evaluate cell proliferation; the comet assay was used to assess DNA damage; and flow cytometry and Western blot analysis were used to clarify the possible regulatory mechanisms in the ACR-induced cell-cycle arrest. Moreover, to clarify the ACR effects on the other human astrocytoma cells, MTT assay and Western blot analysis were also performed by U-251 and U-87 MG cells subjected to ACR treatments. These cell lines were chosen because they are well accepted astrocyte cell models (28–32) and have been used in many investigations of ACR toxicity (16, 17).

Experimental Procedures

Chemicals and Reagents. ACR, dimethyl sulphoxide (DMSO), ethanol, formaldehyde, MTT, propidium iodide, and Triton X-100 were purchased from Sigma-Aldrich (St Louis, MO, USA). Caffeine was purchased from Calbiochem (Gibbstown, NJ, USA). Tris (base) was purchased from J.T. Baker (Phillipsburg, NJ, USA). Tween 20 was purchased from Riedel-de Haen (Seelze, Germany). Skim milk powder was purchased from Anchor (Auckland, NZ). RNase A was purchased from Fermentas (Vilnius, Lithuania). All cell-culture reagents and saline buffers were purchased from Gibco (Rockville, MD, USA). Antibodies against p53, phosphor-p53 (pp53), Ki-67, p21, p27, and actin were purchased from Abcam (Abcam, Cambridgeshire, UK). Cyclin D₁ and cyclin-dependent kinase 2 (Cdk2) were purchased from Cell Signaling Technology (Beverly, MA, USA).

Cell Culture. The human astrocytoma cell lines U-1240 MG, U-251 MG, and U-87 MG were obtained from the Ohio State University (Columbus, OH, USA). All cells were cultured in Dulbecco's modified Eagle's medium with 10% (v/v) heat-inactivated fetal bovine serum (FBS), 100 units/mL penicillin, and 100 µg/mL streptomycin, at 37 °C with 5% CO₂.

Cell Treatments. ACR stock solution (1 M) was prepared with water. Appropriate ACR concentrations in different culture media were measured with care, and all solutions were filter-sterilized before addition to cells. Cell media containing different ACR concentrations (0, 0.5, 1, and 2 mM) were prepared and added to cells. The treated cells were cultured at 37 °C with 5% CO₂ for different time periods (0, 6, 12, 24, 36, and 48 h). To determine the involvement of ATM/ATR in regulating checkpoint-related signals, cells were pretreated with 0, 0.25, 0.5, 1, and 2 mM caffeine for 30 min and were then treated with 2 mM ACR for another 48 h at 37 °C with 5% CO₂.

Cell Proliferation Assay. Cell proliferation was evaluated in three human astrocytoma cell lines by MTT assay. Briefly, cells were plated in a 96-well microtiter plate at a density of 1×10^4 cells per well in a final volume of 200 µL of culture medium. These cells were treated with different ACR concentrations (0, 0.5, 1, and 2 mM) for different time periods (0, 6, 12, 24, 36, and 48 h) at 37 °C with 5% CO₂. After treatment, the cells were immediately incubated with MTT (0.5 mg/mL) for 4 h at 37 °C. The medium was then carefully removed by aspiration, and the cells were lysed in 200 µL of DMSO for 10 min at room temperature. The enzymatic reduction of MTT to formazan crystals that dissolved in DMSO was quantified by Spectra MAX190 photometry (Molecular Devices, Sunnyvale, CA, USA) at 595 nm.

Immunofluorescent Staining. The immunofluorescent staining was carried out according to our previous protocol (17). U-1240 MG cells were grown on 4-well chamber slides (Nunc, Naperville, IL, USA) at 37 °C with 5% CO₂. After treatment with ACR, the cells were washed with PBS three times and then fixed with 3.7% (v/v) formaldehyde in PBS for 15 min. After further washing with PBS three times, the cells were permeated with 0.3% (v/v) Triton X-100 in PBS for 5 min at room temperature. The cells were then incubated with the primary antibody against Ki-67 (1:100; MAB3402, Chemicon, Temecula, CA, USA) in culture medium for 3 h. The

cells were then washed with PBS three times and incubated with the FITC-conjugated rabbit antimouse antibody (1:200; Invitrogen, Grand Island, NY, USA) in culture medium with 0.1% 4, 6-diamidino-2-phenylindole (DAPI) for 45 min. Finally, the cells were washed with PBS three times and then mounted with ProLong Gold antifade reagent (Invitrogen, Grand Island, NY, USA). The signals were observed by a fluorescence microscope (Gmrxa, Leica Microsystems, Germany). Data from 300 representative individual cells were analyzed.

Comet Assay. DNA damage was determined by the comet assay (single-cell gel electrophoresis). Briefly, U-1240 MG cells were treated with different concentrations of ACR for 48 h. Following the treatments, the cells were trypsinized (0.1% trypsin/1 mM EDTA) and counted (1×10^5 cells/mL). The cell suspension was mixed immediately with 1% molten low melting point agarose at 1:10 (v/v) ratio. Cell/agarose mixtures (75 µL) were dropped onto comet slides and incubated in a dark, highly humid environment at 4 °C for 30 min. After solidification, the slides were immersed in prechilled lysis solution (2.5 M NaCl, 100 mM EDTA, 10 mM Tris-HCl, 1% Triton X-100, and 10% DMSO at pH 10.0) and kept at 4 °C for 1 h. The slides were then rinsed with lysis buffer and further immersed in freshly prepared alkaline solution (0.3 N NaOH and 1 mM EDTA) at 4 °C for 1 h to allow DNA unwinding. The slides were rinsed and followed by electrophoresis for 10 min. After electrophoresis, slides were rinsed and incubated with 70% ethanol for 5 min. The samples were air-dried before SYBER green staining. Comet tail lengths were measured under a fluorescence microscope and then analyzed by Northern Eclipse Software (Empix Imaging, North Tonawanda, NY). Representative data from 50 individual cells were analyzed.

Cell-Cycle Analysis. Cell-cycle phase distribution was analyzed by flow cytometry. U-1240 and U-251 MG cells were resuspended in 8 mL of cold ethanol (70%) and stored at –20 °C overnight. To determine cell-cycle profiles, cell samples ($\sim 1 \times 10^6$ cells) were treated with RNase A (0.8 µg/mL) in PBS with 0.5% Triton X-100 at 37 °C for 30 min and incubated in 0.5 mL of PBS with propidium iodide (20 µg/mL) for another 10 min at room temperature in the dark. Finally, cells were analyzed for DNA content with a Beckman Coulter Epic XL-MCL flow cytometer (Beckman Coulter, Miami, FL, USA). The data were analyzed with the Win-MDI (version 2.9) software.

Western Blot Analysis. Antibodies against pp53, p53, p21, p27, cyclin D₁, Cdk2, and actin were used to detect the corresponding protein levels by the immunoblotting method in three astrocytoma cell lines after ACR exposure. After treatment with ACR, total proteins were extracted immediately. Cells were washed with PBS twice and then lysed. Protein samples were harvested in CytoBuster protein extraction reagent (Novagen, Madison, WI, USA) supplemented with 100 µL/mL of protease inhibitor cocktail (Sigma, St Louis, MO, USA). Protein concentrations were determined by a Bio-Rad Laboratories protein assay reagent kit (Hercules, CA, USA). For analysis, the 20 µg of total protein was loaded into a discontinuous 5% stacking and 8% running sodium dodecyl sulfate–polyacrylamide gel (SDS–PAGE). Electrophoresis was performed at 160 V for 40 min; proteins were then transferred to a poly vinylidene fluoride membrane (Bio-Rad Laboratories) at 100 V for 1 h. Thereafter, membranes were blocked in blocking buffer (pH 7.5, 20 mM Tris-buffer saline, 0.05% Tween 20, and 1% powdered skim milk) for 30 min at room temperature. The membrane was then incubated with a primary antibody in the blocking buffer for 2 h at room temperature. The dilutions of pp53, p53, p21, p27, cyclin D₁, Cdk2, and actin were 1:2000, 1:5000, 1:2000, 1:1000, 1:2000, 1:1000, and 1:5000, respectively. The membrane was washed and incubated with a peroxidase-conjugated secondary antibody in blocking buffer for 1 h at room temperature. Protein levels were detected with a Western lighting kit (Perkin-Elmer, Boston, MA, USA) with actin as an internal control. Films were scanned with a Microtek MRX-2400X scanner, and data were quantified with the Multi Gauge V3.0 software (Fujifilm, Stamford, CT, USA).

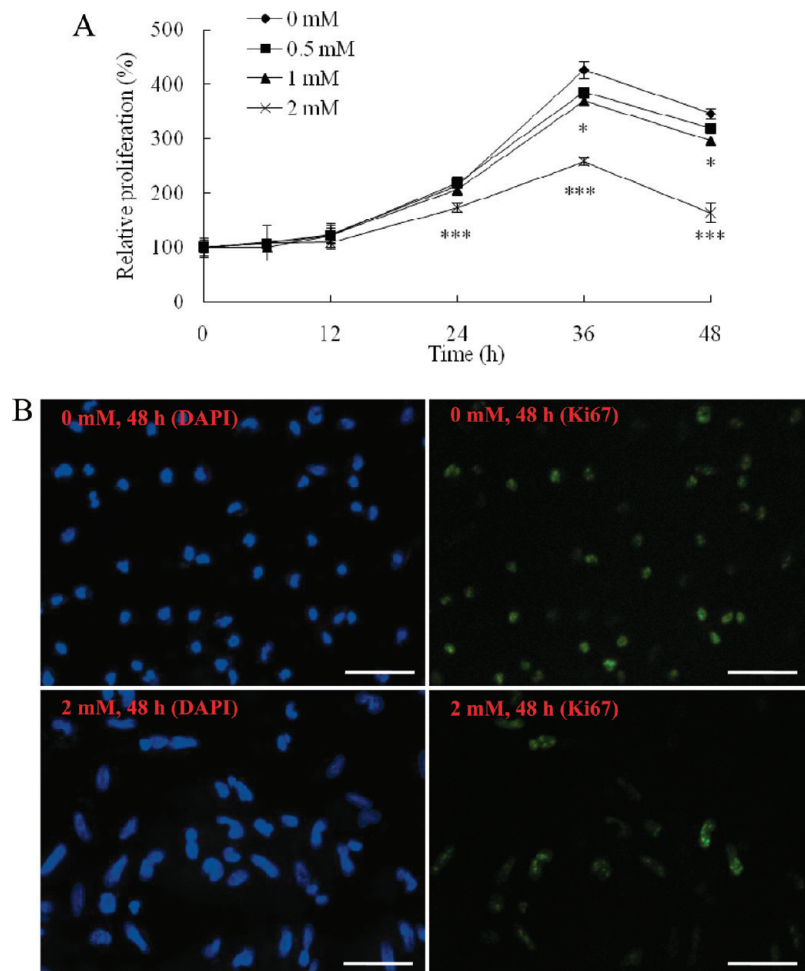


Figure 1. Acrylamide-induced proliferation inhibition of astrocytoma cells in active phases. Acrylamide inhibited the proliferation of the U-1240 MG cells in a time (0, 6, 12, 24, 36, and 48 h)- and concentration (0, 0.5, 1, and 2 mM)-dependent manner when analyzed by MTT assay (A). Ki-67 protein expression in U-1240 MG cells treated with 0 or 2 mM acrylamide for 48 h was analyzed with immunofluorescent staining. DNA was labeled with 0.1% 4,6-diamidino-2-phenylindole (DAPI), and Ki-67 protein was labeled with an anti-Ki-67 antibody (magnification 400 \times , scale bar 80 μ m) (B). Results are presented as the mean \pm SD from three independent experiments (in triplicate for each experiment). Statistical differences to the controls are shown as * p < 0.05, ** p < 0.01, and *** p < 0.001.

Statistical Analysis. Each experiment was performed in triplicate at least three times independently. The data are presented as the mean \pm SD. The statistical significance was determined by the one-way analysis of variance (ANOVA) followed by the Bonferroni multiple comparison test by a statistical package for the social science 13.0 software (SPSS, Chicago, IL, USA). The differences were considered statistically significant when p < 0.05.

Results

Proliferation Inhibition of Astrocytoma Cells at Active Phases. Results from the MTT assay showed that the ACR treatments inhibited the proliferation of U-1240 MG cells in a time- and dose-dependent manner. Significant inhibition was found after exposure to 2 mM ACR for 24 h (Figure 1A; p < 0.001). After treatments for 48 h, the ACR (2 mM) significantly inhibited the cell proliferation by 74% as compared with that by the untreated control (from 346% down to 163%) (Figure 1A; p < 0.001). Ki-67 protein, a reliable proliferation marker for those cells in active phases (G_1 , S, G_2 , and mitosis) of the cell-cycle (33), was chosen to evaluate the proliferation of U-1240 MG cells. As indicated in Figure 1B, cells treated with 2 mM ACR for 48 h caused a significant decrease in cells with positive Ki-67 signals by 45.9% (from 93.7% down to 47.8%) (p < 0.001). These results indicate that the ACR inhibited the proliferation of U-1240 MG cells by arresting the cells in G_0

phase as evaluated by Ki-67 staining. This data was in agreement with our previous report (17), in which the ACR treatments inhibited the proliferation of U-1240 MG cells with no marked necrosis detected.

DNA Damage in U-1240 MG Cells. DNA strand breakage in U-1240 MG cells was evaluated by the comet assay. Figure 2A shows that ACR caused significant increases in DNA migration (p < 0.001) at 48 h. ACR caused increases in tail length (Figure 2B), tail DNA (Figure 2C), and tail moment (Figure 2D) in a dose-dependent manner. These data suggest that ACR induces DNA strand breakage in U-1240 MG cells.

Cell-Cycle Arrest in U-1240 MG Cells. ACR-induced cell-cycle arrest of U-1240 MG cells was analyzed using flow cytometry. A representative cell-cycle profile is shown in Figure 3A. Quantitative analyses of cells in each phase of the cell-cycle following treatment with 2 mM ACR are summarized in Figure 3B. The ACR (2 mM) treatment resulted in significant increases in the G_0/G_1 phase cells (≥ 24 h) and caused significant decreases in the G_2/M phase cells (at 24 h) as well as in the S phase cells (≥ 36 h). Moreover, the cells treated with 0.5, 1, and 2 mM of ACR for 48 h caused significant increases in the G_0/G_1 phase cells by 13.5%, 22.8%, and 14.8%, respectively, with concomitant decreases in both S and G_2/M phases (Figure 3C). These results demonstrate that the ACR treatments of

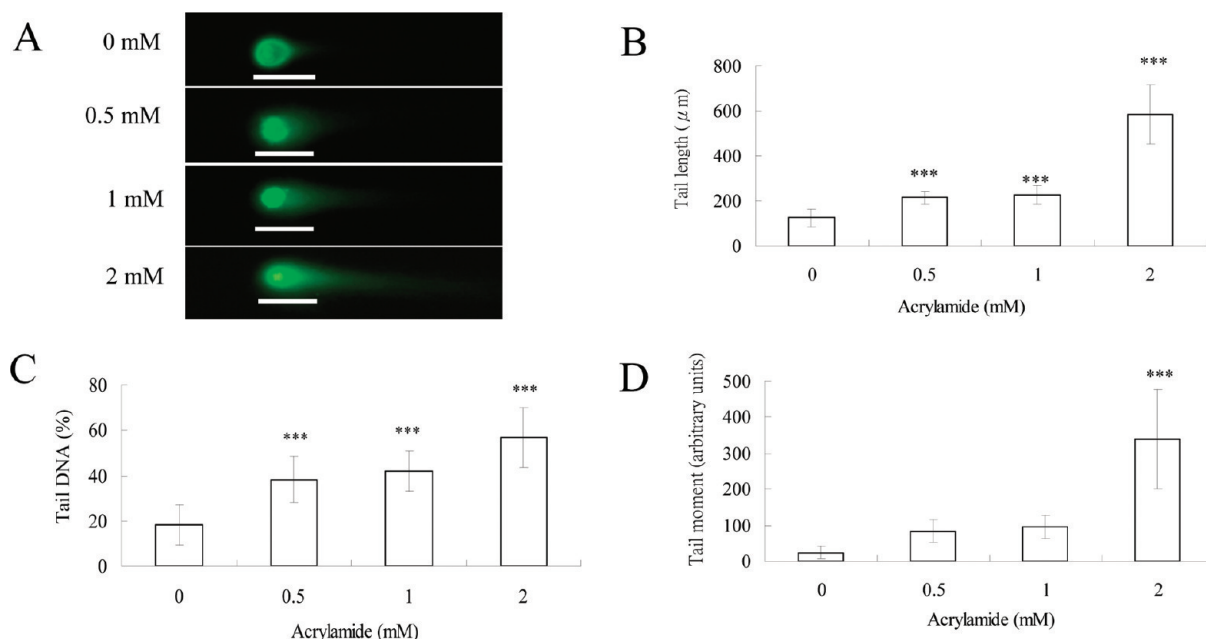


Figure 2. Acrylamide-induced DNA damage in astrocytoma cells. Acrylamide-induced DNA damage in U-1240 MG cells treated with 0, 0.5, 1, and 2 mM acrylamide for 48 h was measured with the comet assay. DNA migration was detected using immunofluorescent staining (A) (magnification 400 \times , scale bar 80 μ m) and was quantified by calculating tail length (B), tail DNA (C), and tail moment (D). Results are presented as the mean \pm SD from three independent experiments (in triplicate for each experiment). Statistical differences to the controls are shown as * p < 0.05, ** p < 0.01, and *** p < 0.001.

U-1240 MG cells may lead to the G₀/G₁ phase arrest in a time- and dose-dependent manner.

Cell-Cycle Regulatory Molecules of U-1240 MG Cells. Following the treatments with 2 mM ACR, levels of the G₀/G₁ cell-cycle control proteins (cyclin D₁ and Cdk2) and the G₀/G₁ arrest checkpoint-related signaling molecules (pp53, p53, p21, and p27) in astrocytes were examined. As shown in Figure 4A, protein levels of pp53, p53, p21, p27, and Cdk2 in U-1240 MG cells increased gradually in a time-dependent manner, whereas cyclin D₁ levels decreased. Moreover, the cells were also subjected to different concentrations of ACR treatments for 48 h. As shown in Figure 4B, treatments with 1 and 2 mM ACR caused significant increases in the protein levels of pp53, p53, and p21. The levels of p27, cyclin D₁, and Cdk2 decreased with increasing ACR exposure concentration (0.5, 1, and 2 mM) at 48 h.

ACR Effects on Proliferation and Cell-Cycle Regulation in Three Astrocytoma Cell Lines. To compare ACR effects on cell proliferation and cell-cycle regulation in different human astrocytoma cells, U-1240 MG, U-251, and U-87 MG cells were treated with 2 mM ACR for 48 h. Results from the MTT assay (Figure 5A) showed that ACR treatments significantly inhibited cell proliferation of all three cell lines. Western blot analyses of cell-cycle regulatory molecules indicated that ACR treatments caused a similar pattern of protein expression in general, with the exception of p53 and p21 in U-251 MG cells (Figure 5B). The induction of p53 protein in U-251 MG cells by ACR showed no significant difference from that in the untreated control. p21 was not detected in either the untreated control or the ACR-treated U-251 MG cells. To overcome this problem, 50 μ g per lane of protein samples were used to detect pp53, p53, and p21 in Western blot analyses. The results in Figure 5C showed that, in response to ACR treatments, U-251 MG cells exhibited different cell-cycle regulatory signals as compared with that of U-1240 and U-87 MG cells. These findings suggest that ACR blocks the cell-cycle progression from G₁ to S phase possibly via the induction of p21 and inhibition of cyclin D₁ in U-1240 and U-87 MG but not in U-251 MG.

Inhibitory Effects of Caffeine on the ACR-Induced Cell-Cycle Arrest. Caffeine has been shown to inhibit ATM and ATR kinase activities (34, 35). This study used caffeine to address the possible involvement of ATM/ATR in the regulation of G₀/G₁ cell-cycle related regulatory molecules of U-1240 MG cells in response to ACR treatments. As shown in Figure 6A, the application of caffeine attenuated the ACR effects on G₀/G₁ cell-cycle related regulatory molecules. Meanwhile, analysis of cell-cycle profiles by flow cytometry revealed that ACR-induced G₀/G₁ phase arrest correlated with decreases in cells in S and G₂/M phases (Figure 6B). Application of caffeine significantly attenuated the ACR-induced G₀/G₁ phase arrest, by 27% (from 77% to 50%) (p < 0.001), with a marked increase in cells in S and G₂/M phases. These results suggest that ACR induces G₀/G₁ phase arrest of astrocytoma cells via the ATM/ATR pathway.

Discussion

The results of the MTT assay and Ki-67 expression suggest that ACR exposure may inhibit the proliferation of astrocytoma cells during the active phases of the cell cycle. ACR-induced cell-growth suppression had been reported in many cell types (10, 23, 24, 36, 37); but the results for astrocytic cell have not been consistent (14–17). As compared with proliferating cell nuclear antigen (PCNA), Ki-67 has been recognized as a more specific indicator for the proliferative activity of human glioblastomas (38–40). Thus, results from the MTT assays and Ki-67 expression using longer exposure times (>24 h) in the current study provide a better correlation between ACR treatments and proliferation inhibition. Aschner et al. reported that ACR promoted astrocytic cell proliferation as seen by the increase in PCNA protein expression (14); the inconsistency of those results with other studies (15–17) may be due to the differences in exposure regimens and/or use of the cell types (rat primary astrocytic cells vs human astrocytoma cell lines). Therefore, the effects of ACR on cell proliferation between primary astrocytic cells and astrocytoma cells remain to be clarified.

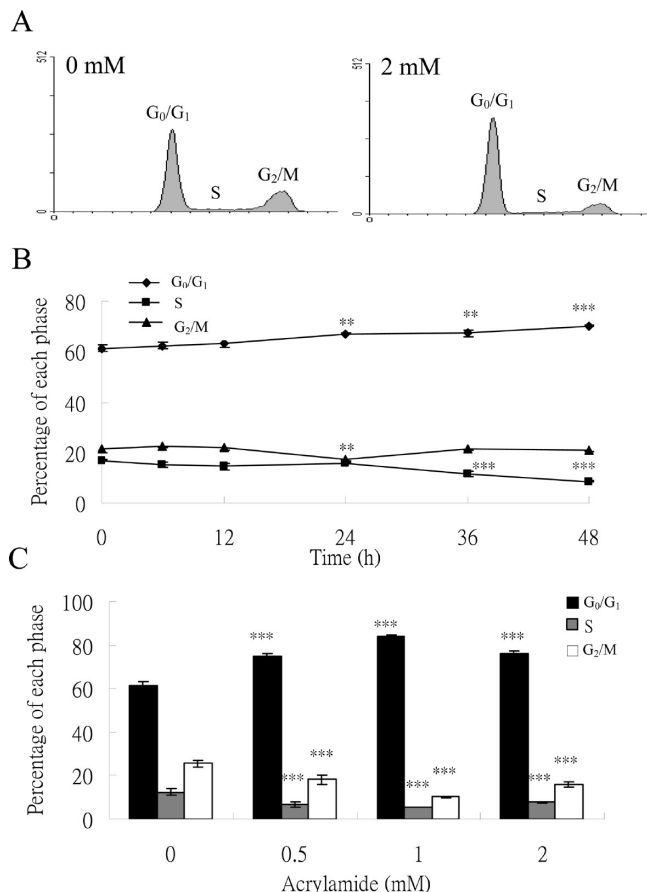


Figure 3. Acrylamide-induced G₀/G₁ cell-cycle arrest in astrocytoma cells. Acrylamide-induced G₀/G₁ phase arrest in U-1240 MG cells treated with acrylamide (2 mM acrylamide for 0, 6, 12, 24, 36, and 48 h, and also by 0, 0.5, 1, and 2 mM acrylamide for 48 h) was analyzed by flow cytometry (A). Quantification data of the cell-cycle (B and C) are expressed as the percentage of each phase and are presented as the mean \pm SD from three independent experiments (in triplicate for each experiment). Statistical differences to the controls are shown as * p < 0.05, ** p < 0.01, and *** p < 0.001.

ACR-induced DNA damage in U-1240 MG was supported by the results of the comet assay, ATM/ATR pathway checkpoint-related signals, and the caffeine attenuated test. The comet assay, which determines DNA damage based on the measurement of DNA migration by electrophoresis as an end point, has been applied to genotoxicity studies (24). ACR is chemically reactive toward nucleophiles, including amino and thiol groups in amino acids and proteins, by Michael additions, but is weakly reactive with the ring nitrogen atoms and the extra-nuclear amino groups of adenine and guanine in DNA (1, 41). However, ACR is easily biotransformed to its epoxide, glycidamide, through cytochrome P450 2E1 (CYP2E1); and glycidamide appears 100–1000 times more reactive with protein and DNA than ACR (42). Because both glycidamide and ACR cause depurinating DNA lesions, the repair of the lesions involves the base excision repair pathway that may lead to the formation of DNA breaks (43, 44). The activation of ATM/ATR kinase in DNA damage responses is involved in the mechanisms of direct activation through interaction with damaged DNA, indirect activation through interaction with DNA repair or maintenance proteins, or a combination of the above (45). Thus, the present study demonstrates that ACR causes DNA damage and ATM/ATR kinase activation in U-1240 MG cells. How the ACR-activated ATM/ATR kinase is involved in apoptosis and DNA repair of astrocytoma cells remains to be elucidated.

Western blot analysis (using 50 μ g protein per lane) showed no detectable levels of CYP2E1 protein in all three astrocytoma cell lines (data not shown). Therefore, ACR-induced genotoxicity in human astrocytoma cells seems to be CYP2E1-independent. However, ACR-induced DNA damage by the comet assay was associated with the generation of intracellular reactive oxygen species (ROS) and 8-hydroxydeoxyguanosine DNA adduct formation in HepG₂ cells (24). In addition, hydroxytyrosol, an efficient scavenger of peroxy radicals, could protect HepG₂ cells from ACR-induced cytotoxicity and DNA damage (36). Taken together, the mechanism of ACR-induced DNA damage in human astrocytoma cells is not associated with the CYP2E1-dependent pathway. The mechanism underlying the generation of intracellular ROS deserves further investigation.

Our data showed that the ACR-induced G₀/G₁ phase arrest of U-1240 MG cells was associated with p21 induction and cyclin D₁ reduction. Cell cycle, determining cell duplication, is regulated by the temporal activation of different Cdk/cyclin complexes (46, 47). In the G₁ phase, the complexes of cyclin D₁/Cdk4/6 and cyclin E/Cdk2 are responsible for the early and the late stages, respectively (48). Cdk inhibitors (CKIs), including p21 and p27, play an important role in arresting the cell-cycle in G₁ phase (49). p21 is induced by p53 in response to DNA-damaging agents and by other transcription factors in p53 negative cells (46, 50). When overexpressed, p21 effectively inhibits Cdk2, Cdk4, and Cdk6 kinases (50). Therefore, the ACR-induced p21 expression could explain, at least in part, the increase of cells arrested in the G₀/G₁ phase by inhibiting cyclin D₁/Cdk4/6 kinase activity.

Regarding cell proliferation and cell-cycle regulatory molecular expression, the three astrocytoma cell lines responded similarly to ACR treatments, except for p53 and p21 expression in U-251 MG cells (Figure 5). Therefore, further examination was taken to clarify whether different responses of cell-cycle arrest were induced by ACR. The results showed that, following ACR treatments, U-251 MG cells were arrested at the G₂/M phase (data not shown), suggesting that the ACR-induced activation of G₂/M DNA damage checkpoints prevents the cells from entering mitosis. In U-251 MG cells, the ACR-induced DNA damage may activate the ATM/ATR kinase and initiate another parallel cascade that inactivates cdc2-cyclin B, a critical complex in the regulation of G₂/M transition (51). These results suggest that ACR-induced cell-cycle arrest (G₀/G₁ or G₂/M) may involve activations of different checkpoint molecules in different human astrocytoma cells.

Our previous study revealed that ACR caused glial fibrillary acidic protein (GFAP) accumulation in astrocytoma cells (17). Elevated expression of GFAP is associated with the toxin-induced astrogliosis in CNS injury (15, 16). Sriram (52) reported that GFAP accumulation was induced through the Janus kinase (JAK)-signal transducer and activator of transcription 3 (STAT3) signaling pathways. STAT3 is a transcription factor that is activated in response to a large number of cytokines, hormones, and growth factors. Because cyclin D₁ is a negative regulator to STAT3 (53), the decreased cyclin D₁ by ACR may activate the JAK-STAT3 signaling pathway and thus lead to GFAP accumulation and astrogliosis. The hypothesis is worth further investigation.

ACR induced p27 expression with time but inhibited p27 expression when ACR concentration was increased; meanwhile, p27 in the control was increasing along the culture period (Figure 4). p27, which is expressed in relatively low levels in many human tumor cells, including U-251 and U-87 MG cells, has a stronger suppression effect on the cell growth of

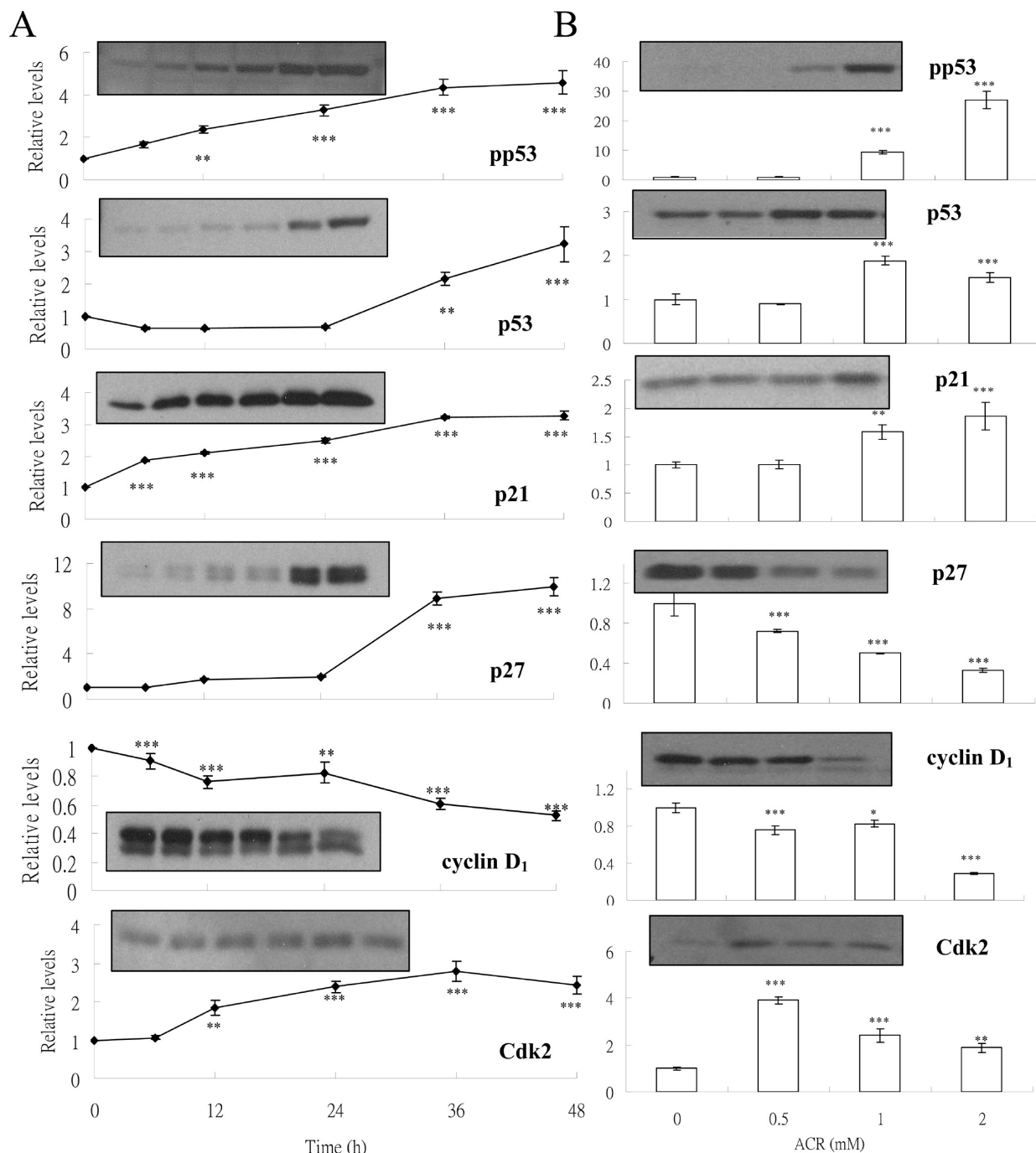


Figure 4. Acrylamide-induced activation of checkpoint-related signaling molecules. Expression of checkpoint-related signaling molecules (pp53, p53, p21, p27, cyclin D₁, and Cdk2) in U-1240 MG cells were measured by immunoblot analysis. The cells were treated with 2 mM acrylamide for different time periods (A) or treated with different concentrations of acrylamide for 48 h (B). The protein levels (mean \pm SD) were normalized by actin protein levels, and then the relative levels were quantified corresponding to 0 h (A) or 0 mM (B). Statistical differences to the controls are shown as * p < 0.05, ** p < 0.01, and *** p < 0.001.

astrocytoma cells than other CKIs (32, 49). In Mv1Lu mink epithelial cells, cell–cell contact arrests the cell-cycle in G₀/G₁ phase by inactivation of the cyclin E/Cdk2 complexes, in which p27 protein binds to and prevents the activation of cyclin E/Cdk2 complexes (54). The present results show that treatment with 2 mM ACR resulted in an inhibition of cell proliferation accompanied by a time-dependent increase in p27 protein. Inhibition of ATM/ATR by caffeine attenuated the ACR-induced inhibition of cell proliferation, though with no marked effect on p27 protein. Therefore, the observed p27 changes in this study might be due to the reduction of cell density rather than due to ACR exposure.

Caffeine, a multiple kinase inhibitor, blocks the ATM/ATR pathway and inhibits the effects of ACR on U-1240 MG cells. We performed a similar set of Western blot and flow cytometry analyses with U-1240 MG cells using a more potent and specific ATM kinase inhibitor-KU-55933 (50 nM) (55). Our results showed that KU-55933 cotreatments did not attenuate the increases in p21, decreases in cyclin D₁, or G₀/G₁ phase arrest by ACR (data not shown). Functional ATM is required for optimal p53 induction and activation following cellular exposure to agents that induce DNA double-strand breaks (26). Moreover, the repair of ACR-induced DNA single-strand breaks involves the base excision repair pathway (43, 44). Therefore, these

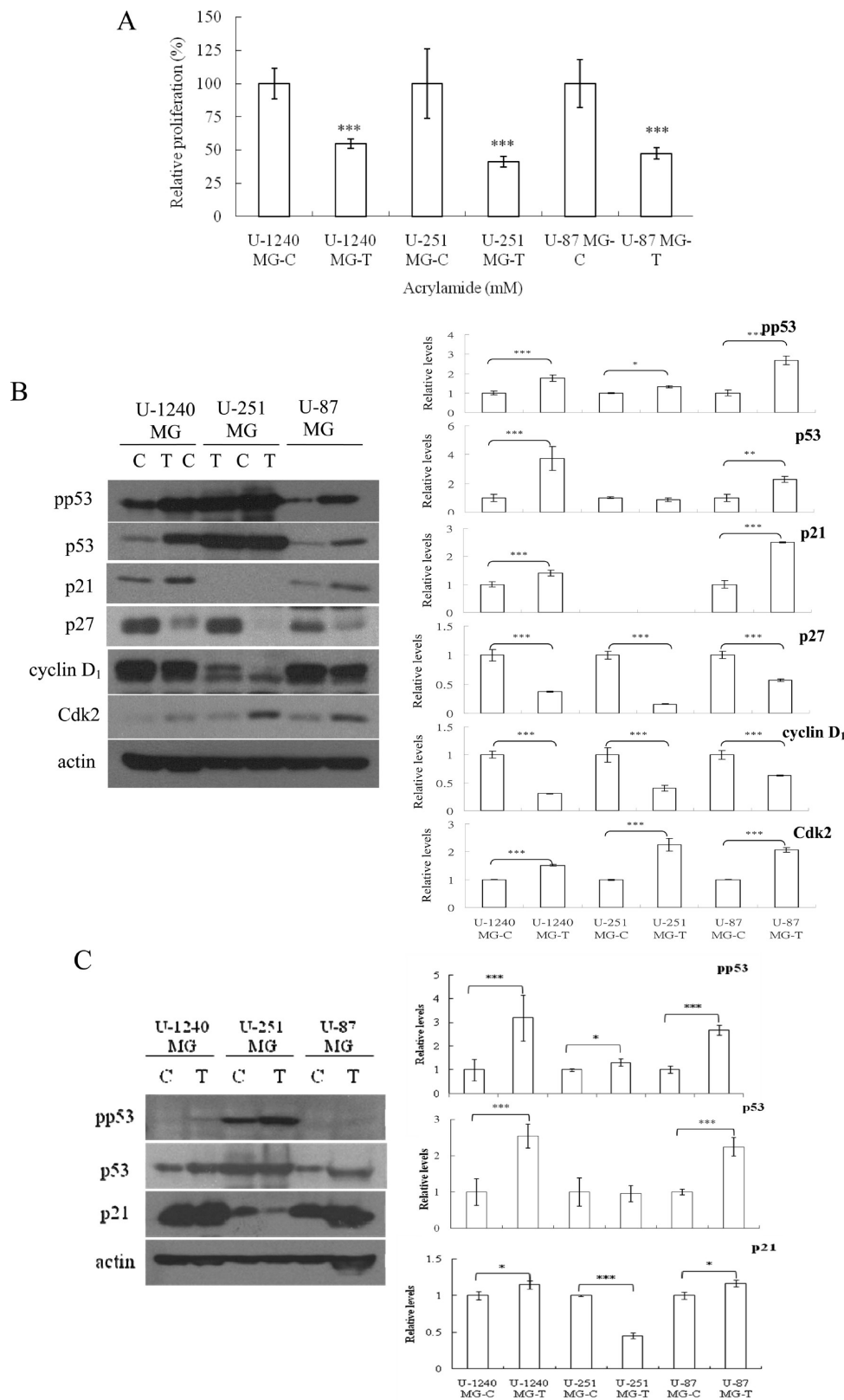
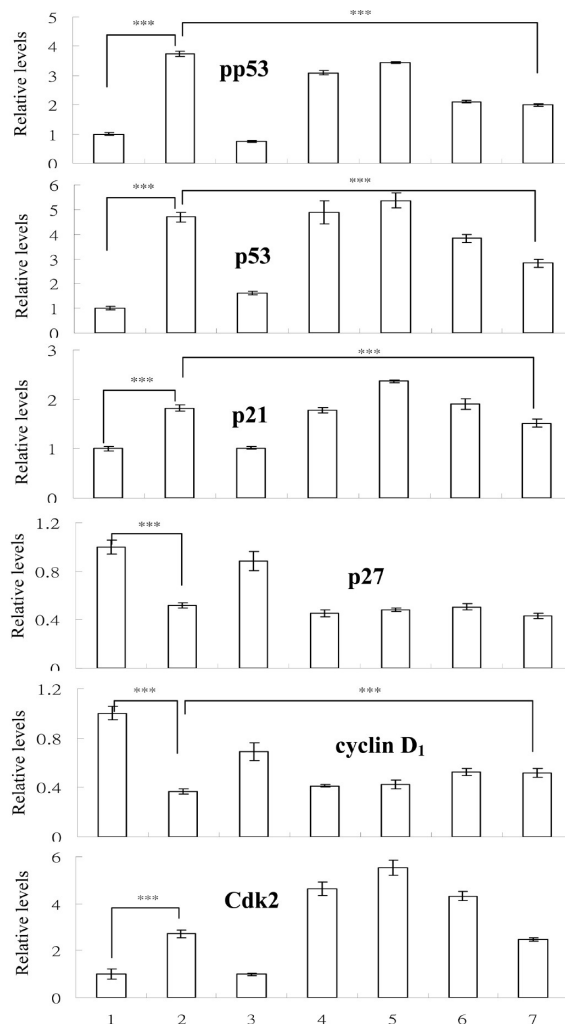
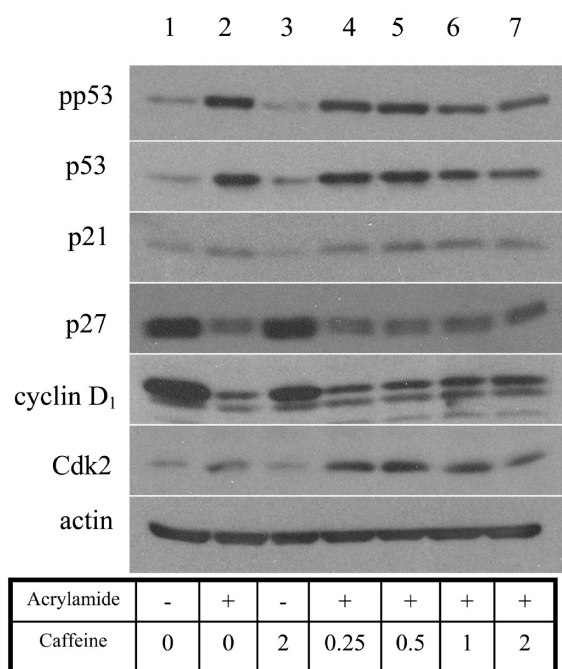


Figure 5. Inhibition of cell proliferation and activation of checkpoint-related signaling molecules in three astrocytoma cell lines (U-1240 MG, U-251 MG, and U-87 MG) treated with acrylamide (2 mM) for 48 h. Inhibition of proliferation was measured with the MTT assay (A). Expression of checkpoint-related signaling molecules (pp53, p53, p21, p27, cyclin D₁, and Cdk2) in the cells treated with 0 mM (C) or 2 mM acrylamide (T) for 48 h was measured with immunoblots (20 μ g of protein per lane) (B). Expression of checkpoint-related signaling molecules (pp53, p53, p21, and cyclin D₁) in the cells treated with 0 mM (C) or 2 mM acrylamide (T) for 48 h was measured with immunoblots (50 μ g of protein per lane) (C). Quantification of protein relative levels was normalized by actin protein levels. Results are presented as the mean \pm SD from three independent experiments (in triplicate for each experiment). Statistical differences to the controls are shown as * p < 0.05, ** p < 0.01, and *** p < 0.001.

A



B

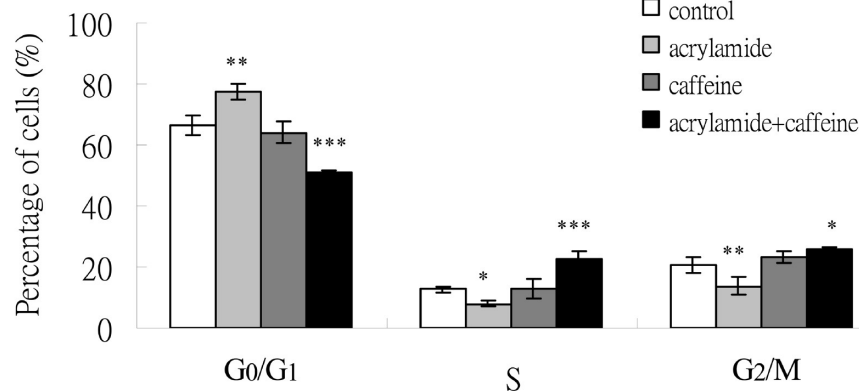


Figure 6. Inhibition of ATM/ATR kinase activity by caffeine-attenuated acrylamide-induced activation of checkpoint-related signals and G₀/G₁ phase arrest. Following pretreatments with different concentrations of caffeine for 30 min, U-1240 MG cells were treated with 0 or 2 mM acrylamide for another 48 h. Effects of caffeine on the expression of checkpoint-related signaling molecules (pp53, p53, p21, p27, cyclin D₁, and Cdk2) were determined with immunoblot analysis (A). Quantification of protein relative levels (mean \pm SD, $n = 3$) was normalized by actin protein levels. Cell-cycle profiles in A were analyzed with flow cytometry (B). Results are expressed as the percentage of each phase and presented as the mean \pm SD ($n = 3$) from three independent experiments (in triplicate for each experiment). Statistical differences to the controls are shown as * $p < 0.05$, ** $p < 0.01$, and *** $p < 0.001$.

results suggest that ACR-induced G₀/G₁ phase arrest of astrocytoma cells was mediated mainly via the ATR kinase.

We previously demonstrated that ACR caused significant astrogliosis (the response of toxin-induced CNS injury using GFAP as a biomarker) and apoptotic responses in astrocytoma cells (17). The present study further showed the significant cytotoxic effects of ACR on U-1240 MG cells. Astrocytes are

responsible for maintaining an optimal microenvironment for neurons and for the integrity of blood–brain barrier (56). On the basis of these studies, we hypothesize that astrocytes exposed to ACR may directly and/or indirectly affect the CNS functions.

In conclusion, this study aimed to determine the *in vitro* effects of ACR on cell proliferation and cell-cycle arrest using human astrocytoma cells, particularly U-1240 MG cells. The

ACR concentrations (0.5, 1, and 2 mM) chosen here were based on the identification of those ACR-induced physiological effectors in astrocytoma cells, including p53 phosphorylation, apoptotic responses, and GFAP accumulation (17). Results from the ACR-treated U-1240 MG cells showed high correlations of cell proliferation inhibition, DNA damage, and G₀/G₁ phase arrest with activations of the ATM/ATR-mediated signaling proteins (p53, pp53, p21, and reduction of cyclin D₁). We also determined the genotoxic effects of ACR-attributed DNA damages in human astrocytoma cells in vitro. U-1240, U-251, and U-87 MG cell lines have common characteristics in cell proliferation inhibition after ACR exposure, whereas U-251 MG exhibits a different p21 protein expression and cell-cycle arrest in G₂/M phase. The ACR concentrations used in this study were higher than those applied in an animal study, in which glial tumors were induced (6). Therefore, the effects of lower concentrations of ACR on the biological outcomes of astrocytic cells remain to be clarified.

Acknowledgment. This work was supported by grants from the National Health Research Institutes in Taiwan. We are grateful to Mr. Mark Swofford for critical editing of the manuscript. We thank Mr. Feng-Yuan Tsai for his excellent technical assistance.

References

- (1) Rice, J. M. (2005) The carcinogenicity of acrylamide. *Mutat. Res.* 580, 3–20.
- (2) Swedish National Food Administration (SNFA) (2002) *Acrylamide Is Formed during the Preparation of Food and Occurs in Many Foodstuffs*, Swedish National Food Administration: Uppsala, Sweden, www.slv.se.
- (3) FAO/WHO (2002) *FAO/WHO Consultation on the Health Implications of Acrylamide in Food, June 25–27. Summary Report*, http://www.who.int/foodsafety/publications/chem/en/acrylamide_summary.pdf.
- (4) Kutting, B., Schettgen, T., Schwegler, U., Fromme, H., Uter, W., Angerer, J., and Drexler, H. (2009) Acrylamide as environmental noxious agent: a health risk assessment for the general population based on the internal acrylamide burden. *Int. J. Hyg. Environ. Health* 212, 470–480.
- (5) International Agency for Research on Cancer (IARC) (1994) *Acrylamide, IARC Monographs on the Evaluation of Carcinogenic Risks to Humans, Some Industrial Chemicals*, Vol. 60, pp 389–433, IARC, Lyon, France.
- (6) Johnson, K. A., Gorzinski, S. J., Bodner, K. M., Campbell, R. A., Wolf, C. H., Friedman, M. A., and Mast, R. W. (1986) Chronic toxicity and oncogenicity study on acrylamide incorporated in the drinking water of Fischer 344 rats. *Toxicol. Appl. Pharmacol.* 85, 154–168.
- (7) Friedman, M. A., Dulak, L. H., and Stedham, M. A. (1995) A lifetime oncogenicity study in rats with acrylamide. *Fundam. Appl. Toxicol.* 27, 95–105.
- (8) Hogervorst, J. G. F., Schouten, L. J., Konings, E. J. M., Goldbohm, R. A., and van den Brandt, P. A. (2009) Dietary acrylamide intake and brain cancer risk. *Cancer Epidemiol. Biomarkers Prev.* 18, 1663–1666.
- (9) Okuno, T., Matsuoka, M., Sumizawa, T., and Igisu, H. (2006) Involvement of the extracellular signal-regulated protein kinase pathway in phosphorylation of p53 protein and exerting cytotoxicity in human neuroblastoma cells (SH-SY5Y) exposed to acrylamide. *Arch. Toxicol.* 80, 146–153.
- (10) Sumizawa, T., and Igisu, H. (2007) Apoptosis induced by acrylamide in SH-SY5Y cells. *Arch. Toxicol.* 81, 279–282.
- (11) Hartley, C. L., Anderson, V. E., Anderton, B. H., and Robertson, J. (1997) Acrylamide and 2,5-hexanedione induce collapse of neurofilaments in SH-SY5Y human neuroblastoma cells to form perikaryal inclusion bodies. *Neuropathol. Appl. Neurobiol.* 23, 364–372.
- (12) Nakagawa-Yagi, Y., Choi, D. K., Ogane, N., Shimada, S. I., Seya, M., Momoi, T., Ito, T., and Sakaki, Y. (2001) Discovery of a novel compound: insight into mechanisms for acrylamide-induced axonopathy and colchicine-induced apoptotic neuronal cell death. *Brain Res.* 909, 8–19.
- (13) Aschner, M., Cao, C., Wu, Q., and Friedman, M. A. (2003) The acute effects of acrylamide on astrocyte functions. *Ann. N.Y. Acad. Sci.* 993, 296–304.
- (14) Aschner, M., Wu, Q., and Friedman, M. A. (2005) Effects of acrylamide on primary neonatal rat astrocyte functions. *Ann. N.Y. Acad. Sci.* 1053, 444–454.
- (15) Cookson, M. R., and Pentreath, V. W. (1994) Alterations in the glial fibrillary acidic protein content of primary astrocyte cultures for evaluation of glial cell toxicity. *Toxicol. in Vitro* 8, 351–359.
- (16) Holden, L. J., and Coleman, M. D. (2007) Assessment of the astroglial responses of three human astrocytoma cell lines to ethanol, trimethyltin chloride and acrylamide. *Toxicology* 241, 75–83.
- (17) Chen, J. H., Wu, K. Y., Chiu, I. M., Tsou, T. C., and Chou, C. C. (2009) Acrylamide-induced astroglial and apoptotic responses in human astrocytoma cells. *Toxicol. in Vitro* 23, 855–861.
- (18) Barres, B. A. (1991) New roles for glia. *J. Neurosci.* 11, 3685–3694.
- (19) Gomes, F. C. A., Paulin, D., and Neto, M. V. (1999) Glial fibrillary acidic protein (GFAP): modulation by growth factors and its implication in astrocyte differentiation. *Braz. J. Med. Biol. Res.* 32, 619–631.
- (20) Lahdetie, J., Suutari, A., and Sjoblom, T. (1994) The spermatid micronucleus test with the dissection technique detects the germ cell mutagenicity of acrylamide in rat meiotic cells. *Mutat. Res.* 309, 255–262.
- (21) Puppel, N., Tjaden, Z., Fueller, F., and Marko, D. (2005) DNA strand breaking capacity of acrylamide and glycidamide in mammalian cells. *Mutat. Res.* 580, 71–80.
- (22) Chico Galdó, V., Massart, C., Jin, L., Vanvooren, V., Caillet-Fauquet, P., Andry, G., Lothaire, P., Dequanter, D., Friedman, M., and Van, S. J. (2006) Acrylamide, an in vivo thyroid carcinogenic agent, induces DNA damage in rat thyroid cell lines and primary cultures. *Mol. Cell. Endocrinol.* 257, 6–14.
- (23) Koyama, N., Sakamoto, H., Sakuraba, M., Koizumi, T., Takashima, Y., Hayashi, M., Matsufuji, H., Yamagata, K., Masuda, S., Kinase, N., and Honma, M. (2006) Genotoxicity of acrylamide and glycidamide in human lymphoblastoid TK6 cells. *Mutat. Res.* 603, 151–158.
- (24) Jiang, L., Cao, J., An, Y., Geng, C., Qu, S., Jiang, L., and Zhong, L. (2007) Genotoxicity of acrylamide in human hepatoma G2 (HepG2) cells. *Toxicol. in Vitro* 21, 1486–1492.
- (25) Keith, C. T., and Schreiber, S. L. (1995) PIK-related kinase: DNA repair, recombination, and cell cycle checkpoints. *Science* 270, 50–51.
- (26) Tibbetts, R. S., Brumbaugh, K. M., Williams, J. M., Sarkaria, J. N., Cliby, W. A., Shieh, S. Y., Taya, Y., Prives, C., and Abraham, R. T. (1999) A role for ATR in the DNA damage-induced phosphorylation of p53. *Genes Dev.* 13, 152–157.
- (27) Levine, A. J. (1997) p53, the cellular gatekeeper for growth and division. *Cell* 88, 323–331.
- (28) Krona, A., Jarnum, S., Salford, L. G., Widegren, B., and Aman, P. (2005) Oncostatin M signaling in human glioma cell lines. *Oncol. Rep.* 13, 807–811.
- (29) Liu, Y., Ray, S. K., Yang, X. Q., Vera, L. L., and Chiu, I. M. (1998) A splice variant of E2–2 basic helix-loop-helix protein represses the brain-specific fibroblast growth factor 1 promoter through the binding to an imperfect E-box. *J. Biol. Chem.* 273, 19269–19276.
- (30) Myers, R. L., Ray, S. K., Eldridge, R., Chotani, M. A., and Chiu, I. M. (1995) Functional characterization of the brain-specific FGF-1 promoter, FGF-1.B. *J. Biol. Chem.* 270, 8257–8266.
- (31) Ray, S. K., Yang, X. Q., and Chiu, I. M. (1997) Transcriptional activation of fibroblast growth factor 1.B promoter is mediated through an 18-base pair cis-acting element. *J. Biol. Chem.* 272, 7546–7555.
- (32) Komata, T., Kanzawa, T., Takeuchi, H., Germano, I. M., Schreiber, M., Kondo, Y., and Kondo, S. (2003) Antitumor effect of cyclin-dependent kinase inhibitors (p16^{INK4A}, p18^{INK4C}, p19^{INK4D}, p21^{WAF1/CIP1} and p27^{KIP1}) on malignant glioma cells. *Br. J. Cancer* 88, 1277–1280.
- (33) Scholzen, T., and Gerdes, J. (2000) The Ki-67 protein: from the known and the unknown. *J. Cell. Physiol.* 182, 311–322.
- (34) Blasina, A., Price, B. D., Turenne, G. A., and McGowan, C. H. (1999) Caffeine inhibits the checkpoint kinase ATM. *Curr. Biol.* 9, 1135–1138.
- (35) Sarkaria, J. N., Busby, E. C., Tibbetts, R. S., Roos, P., Taya, Y., Karnitz, L. M., and Abraham, R. T. (1999) Inhibition of ATM and ATR kinase activities by the radiosensitizing agent, caffeine. *Cancer Res.* 59, 4375–4382.
- (36) Zhang, X., Cao, J., Jiang, L., Geng, C., and Zhong, L. (2009) Protective effect of hydroxytyrosol against acrylamide-induced cytotoxicity and DNA damage in HepG2 cells. *Mutat. Res.* 664, 64–68.
- (37) Oliveira, N. G., Pingarilho, M., Martins, C., Fernandes, A. S., Vaz, S., Martins, V., Rueff, J., and Gaspar, J. F. (2009) Cytotoxicity and chromosomal aberrations induced by acrylamide in V79 cells: Role of glutathione modulators. *Mutat. Res.* 676, 87–92.
- (38) Kayaselcuk, F., Zorludemir, S., Gumurdulu, D., Zeren, H., and Erman, T. (2002) PCNA and Ki-67 in central nervous system tumors: correlation with the histological type and grade. *J. Neuro-Oncol.* 57, 115–121.

- (39) Kordek, R., Biernat, W., Alwasiak, J., and Liberski, P. P. (1996) Proliferating cell nuclear antigen (PCNA) and Ki-67 immunopositivity in human astrocytic tumours. *Acta Neurochir.* 138, 509–512.
- (40) Torp, S. H., and Granli, U. S. (2001) Proliferative activity in human glioblastomas assessed by various techniques. *Acta Pathol. Microbiol. Immunol. Scand.* 109, 865–869.
- (41) Klaunig, J. E. (2008) Acrylamide carcinogenicity. *J. Agri. Food Chem.* 56, 5984–5988.
- (42) Segerbeck, D., Calleman, C. J., Schroeder, J. L., Costa, L. G., and Faustman, E. M. (1995) Formation of N-7-(2-carbamoyl-2-hydroxy-ethyl)guanine in DNA of the mouse and the rat following intraperitoneal administration of [¹⁴C]acrylamide. *Carcinogenesis* 16, 1161–1165.
- (43) Friedberg, E. C., Walker, G. C., and Siede, W. (1995) Base Excision Repair, in *DNA Repair and Mutagenesis* (Friedberg, E. C., Walker, G. C., and Siede, W., Eds.) pp 135–190, American Society for Microbiology, Washington, DC.
- (44) Martins, C., Oliveira, N. G., Pingarilho, M., Costa, G. G., Martins, V., Marques, M. M., Beland, F. A., Churchwell, M. I., Doerge, D. R., Rueff, J., and Gaspar, J. F. (2007) Cytogenetic damage induced by acrylamide and glycidamide in mammalian cells: correlation with specific glycidamide-DNA adducts. *Toxicol. Sci.* 95, 383–390.
- (45) Yang, J., Xu, Z. P., Huang, Y., Hamrick, H. E., Duerksen-Hughes, P. J., and Yu, Y. N. (2004) ATM and ATR: sensing DNA damage. *World J. Gastroenterol.* 10, 155–160.
- (46) Arellano, M., and Moreno, S. (1997) Regulation of CDK/cyclin complexes during the cell cycle. *Int. J. Biochem. Cell Biol.* 29, 559–573.
- (47) Nurse, P. (2000) A long twentieth century of the cell cycle and beyond. *Cell* 100, 71–78.
- (48) Sangfelt, O., Erickson, S., Castro, J., Heiden, T., Gustafsson, A., Stefan, E., and Grander, D. (1999) Molecular mechanisms underlying interferon- α -induced G0/G1 arrest: CKI-mediated regulation of G1 Cdk-complexes and activation of pocket proteins. *Oncogene* 18, 2798–2810.
- (49) Sherr, C. J., and Roberts, J. M. (1999) CDK inhibitors: positive and negative regulators of G₁-phase progression. *Genes Dev.* 13, 1501–1512.
- (50) Jiang, H., Lin, J., Su, Z., Collart, F. R., Huberman, E., and Fisher, P. B. (1994) Induction of differentiation in human promyelocytic HL-60 leukemia cells activates p21, WAF1/CIP1, expression in the absence of p53. *Oncogene* 9, 3397–3407.
- (51) Tsou, T. S., Tsai, F. Y., Yeh, S. C., and Chang, L. W. (2006) ATM/ATR-related checkpoint signals mediate arsenite-induced G₂/M arrest in primary aortic endothelial cells. *Arch. Toxicol.* 80, 804–810.
- (52) Sriram, K., Benkovic, S. A., Hebert, M. A., Miller, D. B., and O'Callaghan, J. P. (2004) Induction of gp130-related cytokines and activation of JAK2/STAT3 pathway in astrocytes precedes up-regulation of glial fibrillary acidic protein in the 1-methyl-4-phenyl-1,2,3,6-tetrahydropyridine model of neurodegeneration. *J. Biol. Chem.* 279, 19936–19947.
- (53) Germain, D., and Frank, D. A. (2007) Targeting the cytoplasmic and nuclear function of signal transducers and activators of transcription 3 for cancer therapy. *Clin. Cancer Res.* 13, 5665–5669.
- (54) Polyak, K., Kato, J. Y., Solomon, M. J., Sherr, C. J., Massague, J., Roberts, J. M., and Koff, A. (1994) p27^{Kip1}, a cyclin-Cdk inhibitors, links transforming growth factor- β and contact inhibition to cell cycle arrest. *Genes Dev.* 8, 9–22.
- (55) Hickson, J., Zhao, Y., Richardson, C. J., Green, S. J., Martin, N. M. B., Orr, A. I., Reaper, P. M., Jackson, S. P., Curtin, N. J., and Smith, G. C. M. (2004) Identification and characterization of a novel and specific inhibitor of the ataxia-telangiectasia mutated kinase ATM. *Cancer Res.* 64, 9152–9159.
- (56) Kramer-Hammerle, S., Rothenaigner, I., Wolff, H., Bell, J. E., and Brack-Werner, R. (2005) Cells of the central nervous system as targets and reservoirs of the human immunodeficiency virus. *Virus Res.* 111, 194–213.

TX1000893